Stellar laboratories

V. The Xe VI ultraviolet spectrum and the xenon abundance in the hot DO-type white dwarf RE 0503−289[*,**]

(Research Note)

T. Rauch[1], D. Hoyer[1], P. Quinet[2,3], M. Gallardo[4], and M. Raineri[4]

[1] Institute for Astronomy and Astrophysics, Kepler Center for Astro and Particle Physics, Eberhard Karls University, Sand 1, 72076 Tübingen, Germany
e-mail: rauch@astro.uni-tuebingen.de
[2] Astrophysique et Spectroscopie, Université de Mons – UMONS, 7000 Mons, Belgium
[3] IPNAS, Université de Liège, Sart Tilman, 4000 Liège, Belgium
[4] Centro de Investigaciones Opticas (CIOp), CC 3, 1897 Gonnet, La Plata, Argentina

ABSTRACT

Context. For the spectral analysis of spectra of hot stars with a high resolution and high signal-to-noise ratio (S/N), advanced non-local thermodynamic equilibrium (NLTE) model atmospheres are mandatory. These are strongly dependent on the reliability of the atomic data that are used for their calculation.
Aims. Reliable Xe VI oscillator strengths are used to identify Xe lines in the ultraviolet spectrum of the DO-type white dwarf RE 0503−289 and to determine its photospheric Xe abundance.
Methods. We publish newly calculated oscillator strengths that are based on a recently measured Xe VI laboratory line spectrum. These strengths were used to consider their radiative and collisional bound-bound transitions in detail in our NLTE stellar-atmosphere models to analyze Xe VI lines exhibited in high-resolution and high S/N UV observations of RE 0503−289.
Results. We identify three hitherto unknown Xe VI lines in the ultraviolet spectrum of RE 0503−289 and confirm the previously measured photospheric Xe abundance of this white dwarf (log Xe = −4.2 ± 0.6 by mass).
Conclusions. Reliable measurements and calculations of atomic data are prerequisite for stellar-atmosphere modeling. Observed Xe VI line profiles in the ultraviolet spectrum of the white dwarf RE 0503−289 were well reproduced with the newly calculated Xe VI oscillator strengths.

Key words. atomic data – line: identification – stars: abundances – stars: atmospheres – stars: individual: RE0503-289 – white dwarfs

1. Introduction

Werner et al. (2012b) identified lines of ten trans-iron elements in the Far Ultraviolet Spectroscopic Explorer (FUSE[1]) observations of RE 0503−289. They were only able to determine the photospheric krypton and xenon abundances because reliable transition probabilities were solely available for these species. New calculations of transition probabilities enabled us in the meantime to measure the abundances of Zn, Ge, Ga, and Ba (Rauch et al. 2014a,b, 2012, 2015, respectively).

Recent measurements of Gallardo et al. (2015) have doubled the spectral information about Xe VI. Since reliable spectral analyses by means of non-local thermodynamic equilibrium (NLTE) model-atmosphere calculations need reliable transition probabilities for the complete model atom (and not only for the identified lines), these new data allow improving the

abundance determination of Xe. Moreover, the many newly classified Xe VI lines enable us to assign hitherto unidentified lines in the observation.

We start with an introduction to our observations and atmosphere models (Sects. 2 and 3). In Sect. 4, we briefly compare the new Xe VI transition probabilities to previous measurements. The line identification and abundance analysis is described in Sect. 5. We summarize the results in Sect. 6.

2. Observations

We analyzed the same FUSE spectrum (910 Å < λ < 1188 Å, resolving power $R = \lambda/\Delta\lambda \approx 20\,000$) that was previously described in detail by Werner et al. (2012b). In addition, we used our recently obtained (and later co-added) *Hubble* Space Telescope/Space Telescope Imaging Spectrograph (HST/STIS[2]) spectra (ObsIds OC7N01010, OC7N01020, grating E140M, 1144 Å < λ < 3073, Å, $R \approx 45\,800$, 2014-08-14, total exposure time of 5494 s). The spectra are available via the Barbara A. Mikulski Archive for Space Telescopes (MAST[3]).

[1] http://fuse.pha.jhu.edu

[2] http://www.stsci.edu/instruments/stis
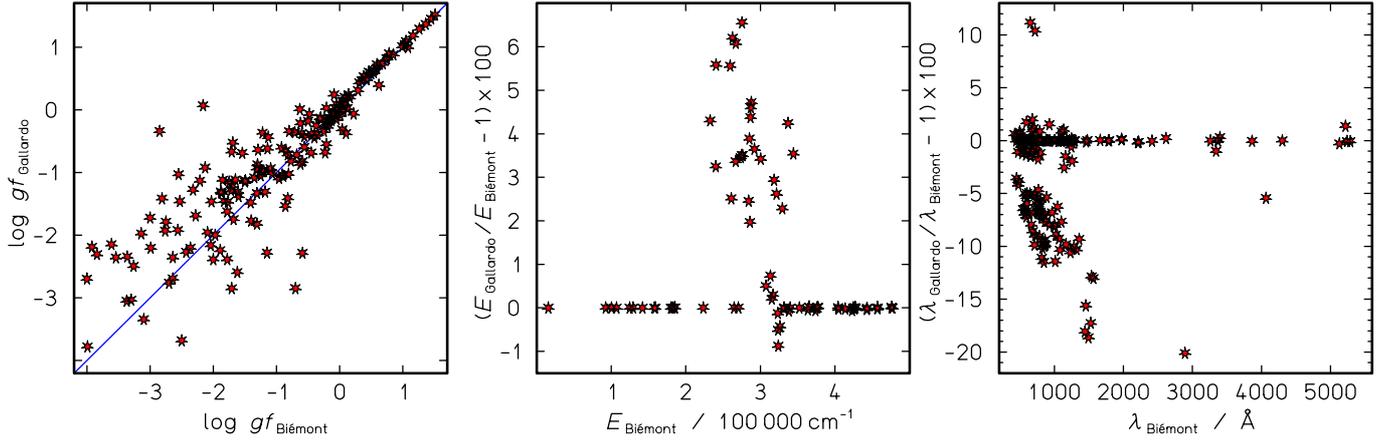[3] http://archive.stsci.edu/

Fig. 1. Comparison of Xe VI data given by Biémont et al. (2005, B+05) and Gallardo et al. (2015, G+15). *Left*: weighted oscillator strengths ($\log gf$) in G+15 as a function of the B+05 values, *middle*: ratio of atomic level energies as a function of the B+05 values, *right*: ratio of line wavelengths as a function of the B+05 values.

3. Model atmospheres

Our model atmospheres are plane-parallel, chemically homogeneous, and in hydrostatic and radiative equilibrium. They are calculated with the Tübingen NLTE Model Atmosphere Package (TMAP[4], Werner et al. 2003, 2012a). Model atoms were constructed from the Tübingen Model Atom Database (TMAD[5], Rauch & Deetjen 2003). TMAD has been constructed as part of the Tübingen contribution to the German Astrophysical Virtual Observatory (GAVO[6]).

4. Xe VI transition probabilities

For their analysis of RE 0503−289, Werner et al. (2012b) used Xe VI data of Reyna Almandos et al. (2001), who used the Hartree-Fock relativistic (HFR) approach to calculate weighted oscillator strengths (gf) of 104 spectral lines belonging to the 5s5p², 5s²5d, 5s²6s, 5s5p5d, 5p³, and 5s5p6s transitions array. In addition, gf-values of an experimental and theoretical study by Biémont et al. (2005) were used. These replaced gf-values of Reyna Almandos et al. (2001) where available. They were calculated for $\Delta n = 0$ and $\Delta n = 1$ transitions connecting the 5s²nl [np (n = 5–8); nf (n = 4–5); nh (n = 6–8); nk (n = 8)], 5s5pnl (nl = 5d, 6s), 5p³, 5s²nl [ns (n = 6–8); nd (n = 5–8); ng (n = 5–6); ni (n = 7–8)], and 5s5p² configurations. Core-polarization (CP) effects were included in their HFR approach. Good agreement was observed between theory and experiment.

Gallardo et al. (2015) observed 243 lines (146 classified for the first time) of the Xe VI spectrum within 400 Å ≤ λ ≤ 5500 Å. They calculated gf-values of 5s5p5d and 5s5p6s configurations. Biémont et al. (2005) encountered a problem in matching the 6d experimental level in their least-squares calculations, which Gallardo et al. (2015, see this paper for further technical details) solved by adjusting configuration interaction (CI) integrals. They achieved standard deviations of 149 cm⁻¹ in the odd parity energies (35 configurations) and 154 cm⁻¹ (34 configurations) in the even parity.

We updated our Xe VI model ion (Werner et al. 2012b) with their experimental level energies (88 levels, 32 classified for the first time, 33 with revised energies) and oscillator strengths (used

Table 1. Comparison of the $\log gf$ values of Xe VI lines calculated by Biémont et al. (2005) and used by Werner et al. (2012b) with those calculated by Gallardo et al. (2015).

Transition		λ/Å	$\log gf$	
			Biémont	Gallardo
5s5p² ²D₃/₂ – 5p³	²D°₃/₂	928.37	−2.11	−0.649
5s5p² ²D₅/₂ – 5p³	²D°₃/₂	967.55	−1.14	−0.937
5s²5p ²P°₁/₂ – 5s5p²	⁴P₃/₂	996.23	−3.37	−3.049
5s²5p ²P°₁/₂ – 5s5p²	⁴P₁/₂	1080.08	−1.64	−1.529
5s²5p ²P°₃/₂ – 5s5p²	⁴P₅/₂	1091.63	−1.25	−1.045
5s5p² ²P₁/₂ – 5p³	²D°₃/₂	1101.95	−2.13	−0.606
5s²5d ²D₅/₂ – 5s²6p	²P°₃/₂	1136.41	+0.06	−0.005
5s²5p ²P°₃/₂ – 5s5p²	⁴P₃/₂	1179.54	−2.09	−1.958
5s²5d ²D₃/₂ – 5s²6p	²P°₁/₂	1181.46	−0.21	−0.226

in the formulae for the cross-sections of radiative and collisional bound-bound transitions). The new Xe VI model ion is available via TMAD.

Figure 1 shows the comparison of the Xe VI $\log gf$ values, level energies, and line wavelengths of Biémont et al. (2005) and the Gallardo et al. (2015). For the strongest lines, that is, $\log gf > 0.0$, the agreement of the oscillator strengths is very good. The energy levels deviate significantly in the 230 000 cm⁻¹ < E < 350 000 cm⁻¹ interval. This results in stronger differences of the lines' wavelengths in the ultraviolet wavelength range ($\lambda < 1700$ Å). The following comparison will verify the quality of the new data.

We start reproducing the lines shown by Werner et al. (2012b). Table 1 shows a comparison of the $\log gf$ values that they used with the new values.

Figure 2 demonstrates how the new oscillator strengths influence the line-profile fits. Because of their much higher $\log gf$ values, Xe VI $\lambda\lambda$ 928.366, 1101.947 Å now match the observation significantly better, while the other lines are almost unchanged. The Xe VII lines are too strong, most likely as a result of our insufficient Xe VII model ion, for which only two oscillator strengths are known (namely of these two lines). In Sect. 5, we search in the FUSE and HST/STIS spectra for further Xe VI lines to evaluate the oscillator strengths.

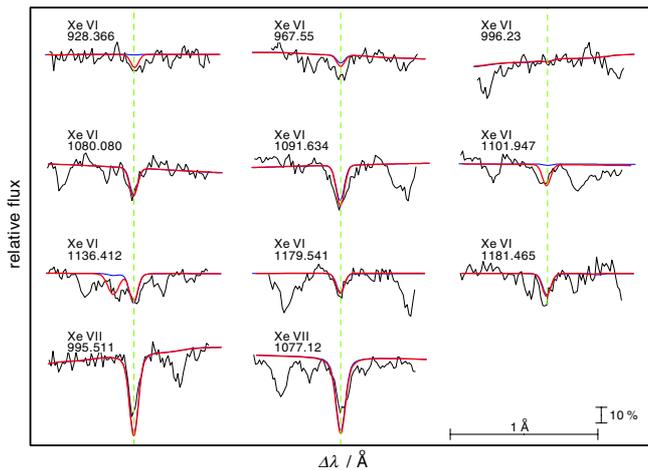[4] http://astro.uni-tuebingen.de/~TMAP
[5] http://astro.uni-tuebingen.de/~TMAD
[6] http://www.g-vo.org

Fig. 2. Xe VI and Xe VII lines calculated from TMAP model atmospheres with $T_{\text{eff}} = 70\,000$ K, $\log g = 7.5$, and $\log$ Xe $= -4.2$ (mass fraction) compared with the FUSE observation. Thin (blue in the online version): model of Werner et al. (2012b), N IV λ 1136.27 Å was not included in the calculation), thick (red) our model. The vertical bar indicates 10 % of the continuum flux level.
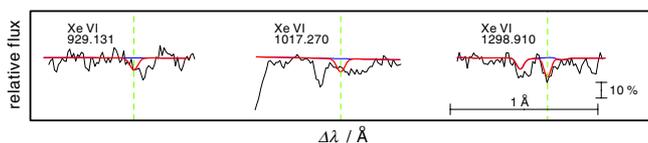

Fig. 3. Xe VI lines calculated from the same models as in Fig. 2 compared with the FUSE and STIS (right panel, Ni V λ 1298.738 Å appears left of Xe VII λ 1298.910 Å) observations. Thin (blue in the online version): model without Xe, thick (red) model including Xe.

5. Line identification and abundance determination

We compared our best model spectra with our FUSE and STIS observations to identify additional Xe VI lines. We found only a few (Fig. 3). Xe VI $\lambda\lambda$ 929.121, 1017, 270 Å have apparently blends with so far unknown lines. Xe VI λ 1298.910 Å matches the STIS observation well. Since all observed Xe lines are reproduced well, we confirm the abundance determination by Werner et al. (2012b), $\log$ Xe $= -4.2 \pm 0.6$. The two identified Xe VII $\lambda\lambda$ 995.511, 1077.12 Å lines (oscillator strengths from Kernahan et al. 1980; Biémont et al. 2007, respectively) are stronger than observed at this abundance (hence the relatively broad error range), but this may be an artifact due to the lack of reliable Xe VII oscillator strengths, cf. Werner et al. (2012b, see Sect. 1 above).

6. Results and conclusions

The recently presented oscillator strengths of Gallardo et al. (2015, 243 lines) complement and improve available data of Reyna Almandos et al. (2001, 104 lines) and Biémont et al. (2005, 491 lines). A comparison of data for lines that are listed in Gallardo et al. (2015) and Biémont et al. (2005) showed that the $\log gf$ values agree well for the strongest lines. Deviations in the line wavelengths are noted, but they do not affect the identified lines in the UV spectra of RE 0503−289 and cannot be
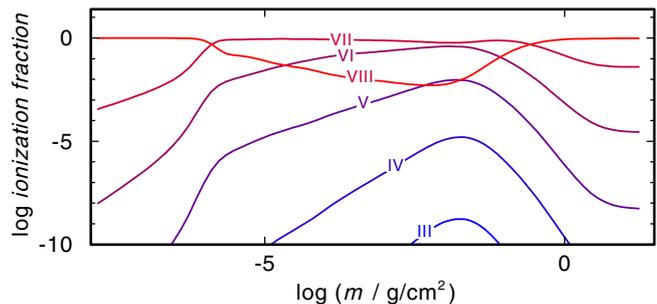

Fig. 4. Xe VI ionization fractions in our best model for RE 0503−289 (Rauch et al. 2015).

assessed. However, a comprehensive recalculation of Xe VI transition probabilities is desirable.

The oscillator strengths of Gallardo et al. (2015) significantly improve the agreement of the synthetic Xe VI line profiles with the observations in two of nine cases. The abundance determination of Werner et al. (2012b, $\log$ Xe $= -4.2 \pm 0.6$) was confirmed.

Figure 4 shows that Xe VII is the dominant Xe ionization stage in the in the line-forming region ($-4 \lesssim \log m \lesssim 0.5$). m is the mass column density, measured from the outer limit of the atmosphere. Therefore, we expect to identify many more Xe VII lines once reliable oscillator strengths for the complete Xe VII model ion are available. This is mandatory to be able to reduce the uncertainty in the Xe abundance analysis.

References

Biémont, É., Buchard, V., Garnir, H.-P., Lefèbvre, P.-H., & Quinet, P. 2005, Eur. Phys. J. D, 33, 181
Biémont, É., Clar, M., Fivet, V., et al. 2007, Eur. Phys. J. D, 44, 23
Gallardo, M., Raineri, M., Reyna Almandos, J., Pagan, C. J. B., & Abrahão, R. A. 2015, ApJS, 216, 11
Kernahan, J. A., Pinnington, E. H., O'Neill, J. A., Bahr, J. L., & Donnelly, K. E. 1980, J. Opt. Soc. Am. (1917−1983), 70, 1126
Rauch, T., & Deetjen, J. L. 2003, in Stellar Atmosphere Modeling, eds. I. Hubeny, D. Mihalas, & K. Werner, ASP Conf. Ser., 288, 103
Rauch, T., Werner, K., Biémont, É., Quinet, P., & Kruk, J. W. 2012, A&A, 546, A55
Rauch, T., Werner, K., Quinet, P., & Kruk, J. W. 2014a, A&A, 564, A41
Rauch, T., Werner, K., Quinet, P., & Kruk, J. W. 2014b, A&A, 566, A10
Rauch, T., Werner, K., Quinet, P., & Kruk, J. W. 2015, A&A, 577, A6
Reyna Almandos, J., Sarmiento, R., Raineri, M., Bredice, F., & Gallardo, M. 2001, J. Quant. Spectr. Rad. Transf., 70, 189
Werner, K., Deetjen, J. L., Dreizler, S., et al. 2003, in Stellar Atmosphere Modeling, eds. I. Hubeny, D. Mihalas, & K. Werner, ASP Conf. Ser., 288, 31
Werner, K., Dreizler, S., & Rauch, T. 2012a, TMAP: Tübingen NLTE Model-Atmosphere Package, Astrophysics Source Code Library
Werner, K., Rauch, T., Ringat, E., & Kruk, J. W. 2012b, ApJ, 753, L7